Inorganic Chemistry

Article

pubs.acs.org/IC

Mechanismic Investigation on the Cleavage of Phosphate Monoester Catalyzed by Unsymmetrical Macrocyclic Dinuclear Complexes: The Selection of Metal Centers and the Intrinsic Flexibility of the Ligand

Xuepeng Zhang,[†] Yajie Zhu,[†] Xiaowei Zheng,[†] David Lee Phillips,[‡] and Cunyuan Zhao*,[†]

[†]MOE Key Laboratory of Bioinorganic and Synthetic Chemistry/KLGHEI of Environment and Energy Chemistry, School of Chemistry and Chemical Engineering, Sun Yat-Sen University, Guangzhou 510275, People's Republic of China

[‡]Department of Chemistry, The University of Hong Kong, Pokfulam Road, Hong Kong, People's Republic of China

Supporting Information

ABSTRACT: The hydrolysis mechanisms of phosphor-monoester monoanions NPP^- (*p*-nitrophenyl phosphate) catalyzed by unsymmetrical bivalent dinuclear complexes are explored using DFT calculations in this report. Four basic catalyst−substrate binding modes are proposed, and two optional compartments for the location of the nucleophile-coordinated metal center are also considered. Five plausible mechanisms are examined in this computational study. Mechanisms 1, 2, and 3 employ an unsymmetrical dizinc complex. All three mechanisms are based on concerted S_N2 addition−substitution pathways. Mechanism 1, which involves more electronegative oxygen atoms attached to the imine nitrogen atoms in the nucleophile-coordinated compartment, was found to be more competitive compared to the other two mechanisms. Mechanisms 4 and 5 are based on consideration of the substitution of the bivalent metal centers and the intrinsic flexibility of the ligand. Both mechanisms 4 and 5 are based on stepwise S_N2-type reactions. Magnesium ions with hard base properties and more available coordination sites were found to be good candidates as a substitute in the M^{II} dinuclear phosphatases. The reaction energy barriers for the more distorted complexes are lower than those of the less distorted complexes. The proper intermediate distance and a functional second coordination sphere lead to significant catalytic power in the reactions studied. More importantly, the mechanistic differences between the concerted and the stepwise pathways suggest that a better nucleophile with more available coordination sites (from either the metal centers or a functional second coordination sphere) favors concerted mechanisms for the reactions of interest. The results reported in the paper are consistent with and provide a reasonable interpretation for experimental observations in the literature. More importantly, our present results provide some practical suggestions for the selection of the metal centers and how to approach the design of a catalyst.

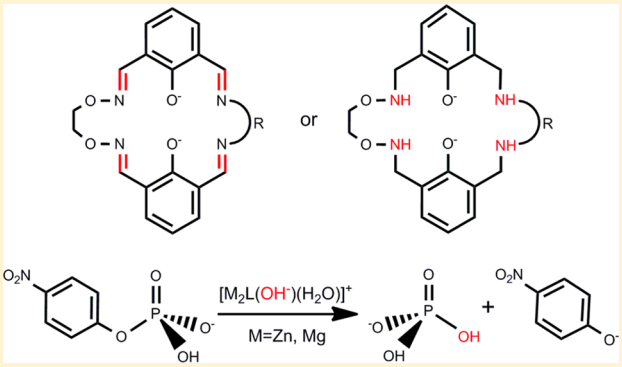

INTRODUCTION

Significant efforts have been made to explore the reaction mechanisms of the solvolytic cleavage of phosphate esters mediated by natural enzymes[1−3] and some metal complexes.[2c,4] As the metabolite of phosphate diesters, phosphate monoesters are widely observed and their kinetic stability prevents further decomposition. The half-life for attack by water molecules on alkyl phosphate dianions is 1.1×10^{12} years ($k = 2 \times 10^{-20}$ s) at room temperature,[5] and phosphatases as well as artificial mimic enzymes especially metal-containing complexes produce significant rate enhancements.

The hydrolysis mechanisms of phosphate diesters catalyzed by metal complexes have been extensively studied. In contrast, a very limited number of experimental and theoretical efforts have been made to study the hydrolytic cleavage of phosphate monoesters.[4a,6−9] In uncatalyzed hydrolysis reactions of phosphor-monoesters, the monoester dianions are acknowledged to undergo a concerted process involving a loose transition state, while the hydrolysis of monoester monoanions is thought to be concerted or to undergo a preassociative mechanism involving a discrete metaphosphate intermediate.[2d,10] In particular, the phosphate monoester dianions are less reactive than the monoanions, and the catalytic advantage of the monoester monoanions is that for the leaving group protonation a proton transfers from the phosphoryl oxygen atom to the leaving group in the P−O bond fission reaction step. However, there are still some uncertainties in the metal-complex-catalyzed hydrolysis mechanisms and the corresponding binding modes of the catalyst−substrate complexes, especially for the phosphate monoester monoanions. During the catalytic process, the proton bound to the phosphoryl oxygen atom may interact with the nucleophile or become involved in the leaving group departure. The rate-limiting step

Received: October 29, 2013
Published: March 21, 2014

   dx.doi.org/10.1021/ic402717x | *Inorg. Chem.* 2014, 53, 3354−3361

of the enzymatic reaction is not clear yet. Proton transfer, nucleophilic attack, P−O bond cleavage, or nonchemical steps could be rate-determining steps.[6b] It is difficult to solve these mechanistic issues via conventional experimental approaches, and thus theoretical efforts are helpful to explore this issue.

Meanwhile, the selection of the metal centers is quite important in the design of chemical mimics of enzymes. In particular, bivalent metal centers such as zinc(II) and magnesium(II) ions with appropriate Lewis acidity, rapid ligand exchange, nontoxicity, inert reduction character, and a wide range of coordination number are preferred and popular choices for the metal centers.[2a,4e,10a,11,12] Compared with zinc(II) ions, magnesium(II) ions are hard acids in nature, and thereby, the linkages between the hard base coordination atoms and the magnesium(II) centers are slightly stronger than the zinc-bound centers. The zinc centers are generally pentacoordinated in the stable reaction species, while magnesium ions prefer a hexacoordinated configuration.[12] The hard acid properties as well as having more available coordination sites might lead to different reaction mechanisms in these two types of metal center systems, and it is helpful to utilize computational methods to study the reaction mechanisms and compare them.

In general, it is noted that binuclear metal complexes are more effective and reactive than their mononuclear counterparts.[6c,13] Kandaswamy and co-workers[9c] used a series of oxyimine-based macrocyclic dinuclear zinc(II) complexes in combination with 4-nitrophenyl phosphate (NPP) to investigate the hydrolysis mechanisms of these systems. An unsymmetrical macrocyclic dinuclear zinc(II) complex $[Zn_2L^6]^{2+}$ with 1,8-diamino naphthalene was synthesized and exhibited impressive catalytic activity. Unsymmetrical dinuclear metal complexes with two different metal-containing compartments have altered intermetallic distances that are more interesting but much more challenging to calculate than similar symmetrical complexes for the catalytic processes involved in the hydrolysis reactions. Previous research on unsymmetrical[9b,14] dinuclear mimic enzymes have revealed the catalytic benefit of these unsymmetrical pathways for some reactions. However, the mechanistic differences of the unsymmetrical catalyst involved reactions, including the location of the nucleophile reagent and the cooperative functions of the bimetal centers during the catalytic process, have not been well explored. The intrinsic rigidity of the ligand ring directly influences the flexibility of the geometry around the metal centers and the corresponding intermetallic distance. The change of the intrinsic rigidity of the ligand can significantly influence the catalytic power of the reaction system.[15] Meanwhile, noncovalent interactions in the second coordination spheres of the catalysis system play an important role in recognition and selectivity, and thereby, a clear description can be instructive to the complex natural enzymatic systems.[4g,i,6c,11c,d] Herein, we attempt to obtain a more detailed understanding of the catalytic mechanisms of the cleavage of NPP mediated by unsymmetrical dinuclear bivalent metal complexes by employing density functional theory (DFT) calculations to study these kinds of reactions (Scheme 1).

EXPERIMENTAL SECTION

All of the calculations were performed with the Gaussian 09 program[16] using density functional theory. In our previous work,[17] a functional comparison was made, and the B3LYP[18] functional, which has a lower computational expense and a better agreement with experimental

Scheme 1. Schematic Depiction of the Hydrolysis Reaction of NPP Catalyzed by Unsymmetrical Dinuclear Bivalent Metal Complexes

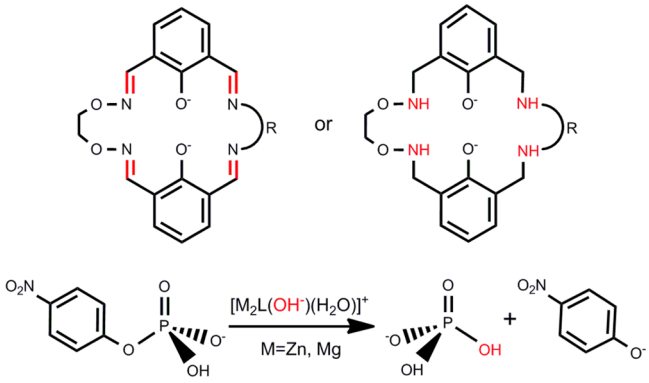

observations, was demonstrated to be sufficient to describe several phosphate ester hydrolysis reactions.[4h,17] Therefore, the B3LYP hybrid functional has been adopted to study the reactions of interest in this work as well. Polarized basis sets 6-31G(d, p) (for the C, H, and Mg atoms), diffused basis sets 6-31+G(d, p) (for the O, N, and P atoms), and Stuttgart/Dresden (SDD) basis sets with the effective core potential[19] (for the zinc atoms) were employed in the optimization procedure of the calculations. Frequency calculations were conducted to obtain thermodynamic data and to distinguish transition states from local minima. All the transition states are confirmed by the intrinsic reaction coordinate (IRC)[20] method with the HPC[21] algorithm. Subsequently, diffusion functional basis sets 6-311++G(d, P) (for the C, H, O, N, P, and Mg atoms) in combination with SDD basis sets (for the Zn atoms) were utilized to refine the energy of the reaction complexes. An implicit solvation model was employed to estimate the solvation energies in aqueous solution by utilizing the polarized continuum model (PCM):[22] more explicitly, a PCM model with Bondi[23] atomic radii, a PCM model with UFF[23] atomic radii, and an SMD[24] model in the calculations. Calculations in solution are single-point energy evaluations without further reoptimization in order to keep the computations tractable for our computational resources. The nonelectrostatic terms were taken from the SMD model calculations. All of the thermodynamic data were obtained at 298.15 K.

RESULTS AND DISCUSSION

Active Catalysts. Zinc(II) ions are generally pentacoordinated in aqueous solution,[2,4] and thereby, each zinc(II) ion in the unsymmetrical complex initially possesses an axially coordinated water molecule. The pK_a value of the zinc-bound water molecule is 6.5,[9c] and the pH value of the reaction system is maintained at 7.5. Therefore, the Zn-bound water molecule might be deprotonated at this pH condition. In addition, the electronegative phosphate substrate can be easily recognized and bond with an electropositive complex. Meanwhile, the metal-bound water molecule or hydroxide can be either above or below the catalyst plane. Finally, the active catalyst is obtained as *trans*-$[Zn_2L^6(H_2O)(OH^-)]^+$ in consideration of the catalytic benefit of its electropositivity and steric hindrance.

Binding Modes of the Catalyst−Substrate Complexes. The axially coordinated water molecule in the active catalyst *trans*-$[Zn_2L^6(H_2O)(OH^-)]^+$ is likely to dissociate to the solution when a substrate attacks the catalyst plane. The phosphate ester can bind with the catalyst by either one coordination linkage or two coordination bonds. Besides, one or two hydrogen bonds can be formed between the hydroxide and the substrate NPP^-. Meanwhile, the hydroxide ion can be bridged or bound to a metal center either in close proximity to

dx.doi.org/10.1021/ic402717x | Inorg. Chem. 2014, 53, 3354−3361

Scheme 2. Location of the Nucleophile-Bound Metal Center and the Four Basic Catalyst–Substrate Binding Modes

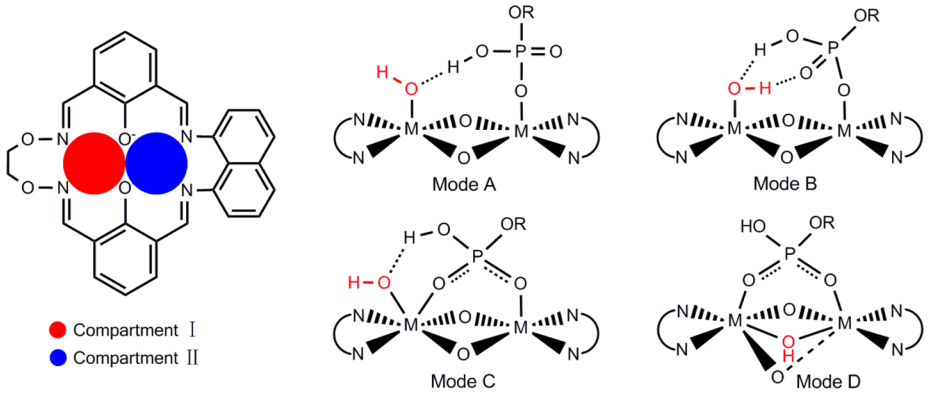

Scheme 3. Schematic Representations of the Proposed Mechanisms 1, 2, and 3 for the NPP^- Cleavage Promoted by Unsymmetrical Dizinc(II) Complexes

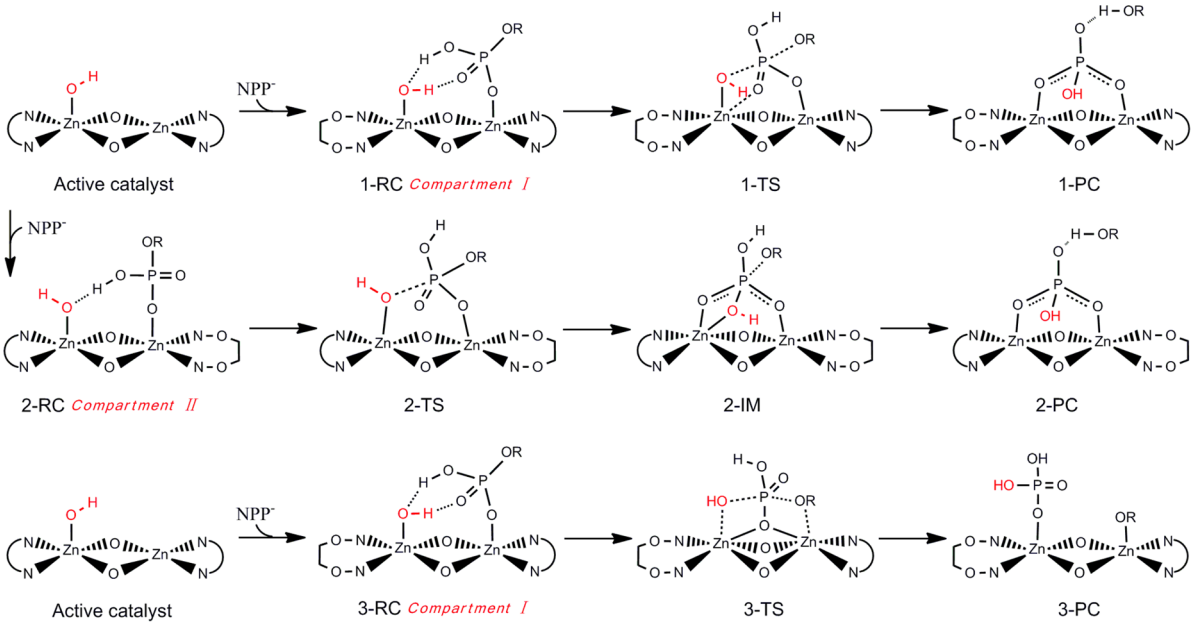

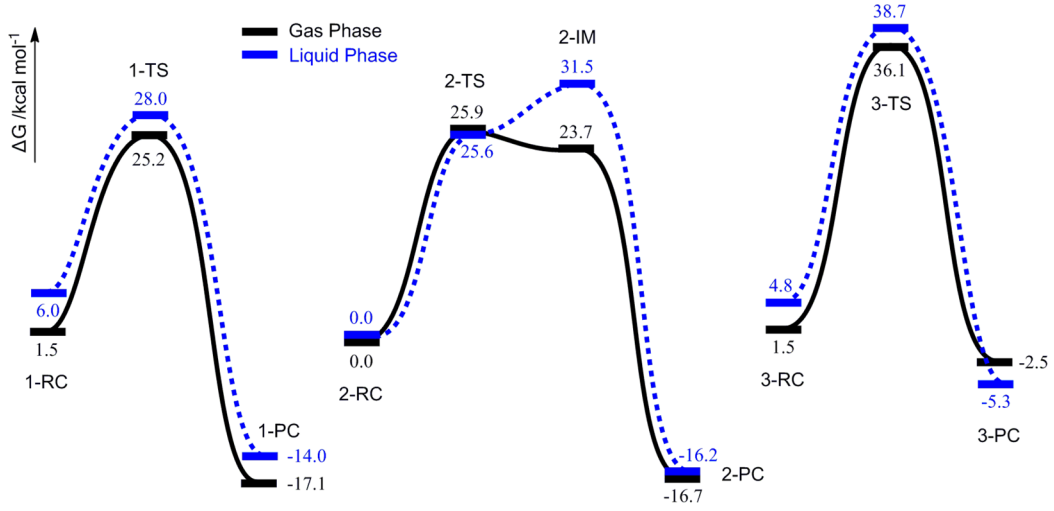

Figure 1. Relative free energy profiles of mechanisms 1, 2, and 3. The relative free energies of **2-RC** (based on mode A) in both the gas phase and the liquid phase are set to zero.

dx.doi.org/10.1021/ic402717x | *Inorg. Chem.* 2014, 53, 3354–3361

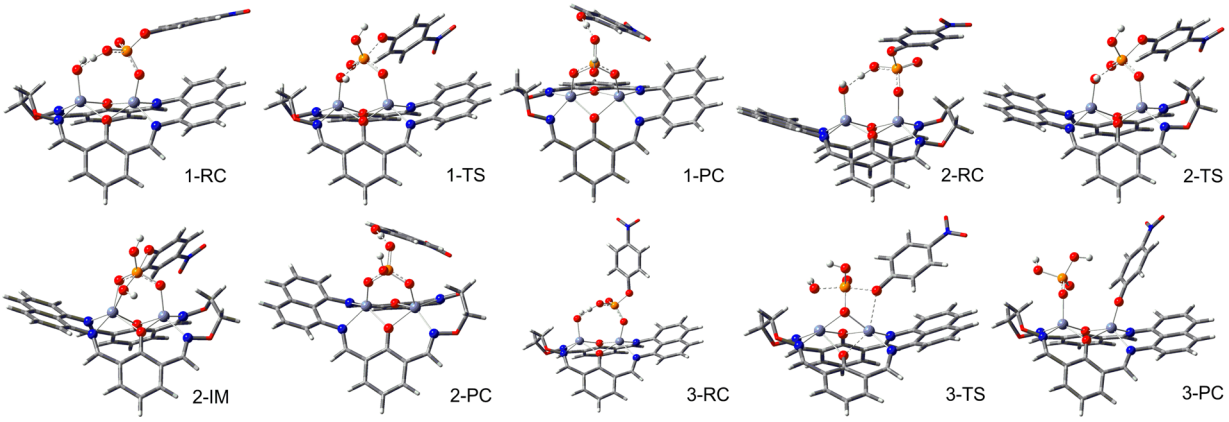

Figure 2. Optimized structures of the stationary reaction species in mechanisms 1, 2, and 3.

1,8-diaminonaphthalene or in the other compartment. Finally, four basic binding modes without consideration of the location of the nucleophile are obtained (Scheme 2). In modes A, B, and C, the nucleophile hydroxide ion can be located in either compartment I or compartment II. Therefore, seven plausible catalyst−substrate binding modes (including mode D) are obtained. As has been mentioned above, the zinc(II) centers are not very stable when hexacoordinated. Therefore, only modes A and B are considered in the zinc-contained reaction systems, and all of the binding modes are modeled in the magnesium-containing systems. Both modes A and B adopt a one-point binding mechanism[9e] in which one metal center is coordinated with the substrate, while the other metal center is occupied by the nucleophile hydroxide. A two-point binding mechanism[25] is adopted in both modes C and D, and one metal center in mode C is hexacoordinated, while the hydroxide ion in mode D is bridged.

Mechanisms for the Hydrolysis of NPP Catalyzed by Dinuclear Metal Complexes. Five main reaction mechanisms are discussed in this paper and the less favored mechanisms are also provided in the Supporting Information.

Mechanisms 1, 2, and 3. These proposed reaction mechanisms are presented in Scheme 3, and the potential energy surface (PES) profiles and the corresponding optimized reaction structures are depicted in Figures 1 and 2, respectively. As has been discussed above, only modes A and B are considered to model the catalyst−substrate binding modes in the case of the dizinc centers combined with the aromatic rigid ligand L[6]. The nucleophile-coordinated metal center in either mechanism 1 or mechanism 3 is located at compartment I, while compartment II is chosen in mechanism 2. Both reactant complexes **1-RC** and **3-RC** are modeled based on mode B, while **2-RC** is constructed based on mode B.

Mechanism 1 is a concerted S_N2-type addition−substitution reaction pathway. In **1-RC**, two hydrogen bonds are generated between the nucleophile and the substrate. The coordination linkage between the catalyst and the substrate activates the substrate by an electron transfer from the phosphorus center in the substrate to a metal center in the catalyst. Subsequently, the electropositive phosphorus center can be easily attacked by the metal-bound nucleophile hydroxide ion, and a distorted trigonal bipyramidal phosphorane transition state, **1-TS**, is formed. In **1-TS**, both bond formation to the nucleophile and bond fission to the leaving group take place. A hydrogen bond exists between the oxygen atom in the leaving group and the phosphoryl oxygen-bound proton. The P−O bond to the leaving group appears to cleave concurrently with the protonation of the leaving group. The catalytic benefit of the leaving group protonation is a major reason for NPP^- exhibiting a greater activity than NPP^{2-}.

Mechanism 2 is similar to mechanism 1 in the way the nucleophilic attack occurs except that a reaction intermediate, **2-IM**,[26] is formed in mechanism 2. In **2-TS**, the P---O distance to the nucleophile and the leaving group is 2.18 and 1.80 Å, respectively. These distances indicate that the transition state **2-TS** locates more closely to the reactant, and mechanism 2 has a concerted, asynchronous S_N2-type reaction pathway character. Why does a reaction intermediate exist in mechanism 2? The location of the nucleophile-coordinated metal center is the reason for this intermediate to be present. In **1-RC**, the nucleophile-coordinated zinc(II) center is located in compartment I with more electronegative oxygen atoms attached to the imine nitrogen atoms, which strengthens the coordination linkages between the zinc(II) center and the imine nitrogen atoms while weakening the linkage between the zinc(II) center and the nucleophile hydroxide ion. This indicates that the nucleophilic ability of the hydroxide ion is strengthened in compartment I, and thereby, a concerted pathway is found in mechanism 1.

Mechanism 3 is also an S_N2-type addition−substitution reaction but in a substantially different way. Both **1-RC** and **3-RC** are modeled based on mode B, while the orientations of the *p*-nitrophenyl leaving groups are different. The aromatic leaving group can be inclined either toward (**1-RC**) or away from (**3-RC**) the catalyst plane, and the latter configuration would hinder the formation of a hydrogen bond between the leaving group and the phosphoryl oxygen-bound proton in the subsequent transition state **3-TS**. In **3-TS**, one phosphoryl oxygen atom is coordinated with both zinc(II) centers, while the other one is exposed to the solution. This kind of coordination configuration can also be seen in the putative transition states in alkaline phosphatase,[3d] ribonuclease,[3b] and inositol monophosphatase[10a] active sites. The P−O bonds to the nucleophile and leaving group are 1.83 and 1.92 Å, respectively. These bond lengths indicate a tendency for P−O bond formation to the nucleophile and bond fission to the leaving group. Unlike **1-TS** and **2-TS**, the catalytic benefit of the leaving group departure in **3-TS** is a metal-induced mechanism in which the electronegative oxygen atom in the leaving group is attracted by an adjacent metal center and finally the leaving group is dissociated to the catalyst.

dx.doi.org/10.1021/ic402717x | *Inorg. Chem.* 2014, 53, 3354−3361

Inspection of Figure 1 shows that mechanism 1 is the most favored pathway among the three proposed mechanisms. It turns out that the compartment with the more electronegative atoms attached to the coordination atoms prefers to bind a nucleophile. Meanwhile, the protonation of the leaving group is more favorable than a metal-induced leaving group departure. In addition, the reaction starting materials are dissociative catalysts and substrates, and the activation free energy of mechanism 1 is 18.5 kcal/mol when the sum of free energies of the dissociative catalyst and substrate is set to zero. The experimental value of the activation free energy is 19.6 kcal/mol. Therefore, our calculated results are consistent with the experimental observations and, more importantly, illuminate the mechanistic differences in the hydrolysis reactions catalyzed by the unsymmetrical dinuclear metal complexes.

PCM models with Bondi atomic radii and UFF atomic radii and the SMD model are utilized in our calculations that include the effect of solvation (Table 1). Inspection of these results in

Table 1. Calculated Relative Free Energies of the Reaction Species in Mechanism 1 and Mechanism 2 in the Liquid Phase Using Different PCM Keywords: SMD, Bondi, and UFF

term	1-RC	1-TS	1-PC	2-RC	2-TS	2-IM	2-PC
SMD	6.0	28.0	−14.0	0.0	25.6	31.5	−16.2
Bondi	5.3	29.1	−13.9	0.0	26.8	30.8	−15.7
UFF	4.1	29.5	−14.1	0.0	27.6	29.6	−15.5

Table 1 shows that the calculated values determined from the three methods are very close to each other. Hence, the SMD (including nonelectrostatic terms) results are finally used for the sake of computational simplicity.

Mechanism 4. Magnesium(II) ions rather than zinc(II) ions are considered in mechanism 4. As mentioned above, magnesium(II) ions are inclined to be pentacoordinated or hexacoordinated during the catalytic processes. Therefore, four basic catalyst−substrate binding modes are considered in the magnesium-containing system (see results in the Supporting Information), and the results indicate that the mode A based complex is the most stable catalyst−substrate binding complex. Similarly, the favorable nucleophilic attack pattern in mechanism 1 is adopted for the sake of computational simplicity. The proposed mechanisms are presented in Scheme 4. The PES profiles and corresponding optimized structures are shown in Figures 3 and 4, respectively.

Unlike the zinc-containing mechanism 1, mechanism 4 is a stepwise S_N2-type addition−substitution reaction pathway. In **4-TS1**, both of the phosphoryl oxygen atoms are coordinated with two metal centers, respectively, and the nucleophile-coordinated magnesium center is hexacoordinated. The P−O bond to the nucleophile is further strengthened, and a less distorted trigonal bipyramidal phosphorane intermediate, **4-IM**, is obtained. Subsequently, the P−O bond to the leaving group gets elongated simultaneously with the further formation of the P−O bond to the nucleophile, resulting in a second transition state, **4-TS2**, along the reaction coordinate. Finally, the P−O bond to the leaving group is cleaved and the protonated leaving group is dissociated into the solution. Why is mechanism 1 concerted while mechanism 4 is a stepwise pathway? This mechanistic difference is ascribed to the availability of the coordination sites of the metal centers. Hexacoordinated magnesium(II) centers are quite stable, which indicates that the reaction species, especially the transition states and intermediates, can be well stabilized. Hence, mechanism 4 is a stepwise pathway due to the availability of more coordination sites.

It can be seen from Figure 3 that the reaction barrier of mechanism 4 is 26.0 kcal/mol, which is lower than that in mechanism 1 (28.0 kcal/mol). This indicates that magnesium(II) ions with hard base properties and more available coordination sites are a good candidate as a substitute for M^{II} dinuclear phosphatases. Evidence can be found in alkaline phosphatases.[12b,c]

Mechanism 5. As mentioned above, variation of the intrinsic rigidity of the ligand can influence the catalytic power of the catalyst.[15] In Kandaswamy and co-workers' work,[9c] the flexibility of the catalyst was altered by changing the ligand ring size. However, the coordination environments for the metal centers are modestly influenced due to the significant intrinsic rigidity of the aromatic ligand. In the system examined here, the aromaticity of the ligand is partly broken via replacing the imine groups with amines (Scheme 5). This process is synthetically feasible via a Borch reduction with a mild reductant such as sodium tetrahydridoborate or sodium cyanoborohydride. For brevity, this new unsymmetrical macrocyclic ligand is named $L^{6\prime}$. Mechanism 5 is proposed using the active catalyst *trans*-$[Zn_2L^{6\prime}(H_2O)(OH^-)]^+$. This reaction scheme is presented in Scheme 4. The PES profiles and optimized structures are depicted in Figures 3 and 4, respectively.

Scheme 4. Proposed Mechanisms 4 and 5 for the NPP^- Cleavage Promoted by Unsymmetrical Bivalent Dinuclear Complexes

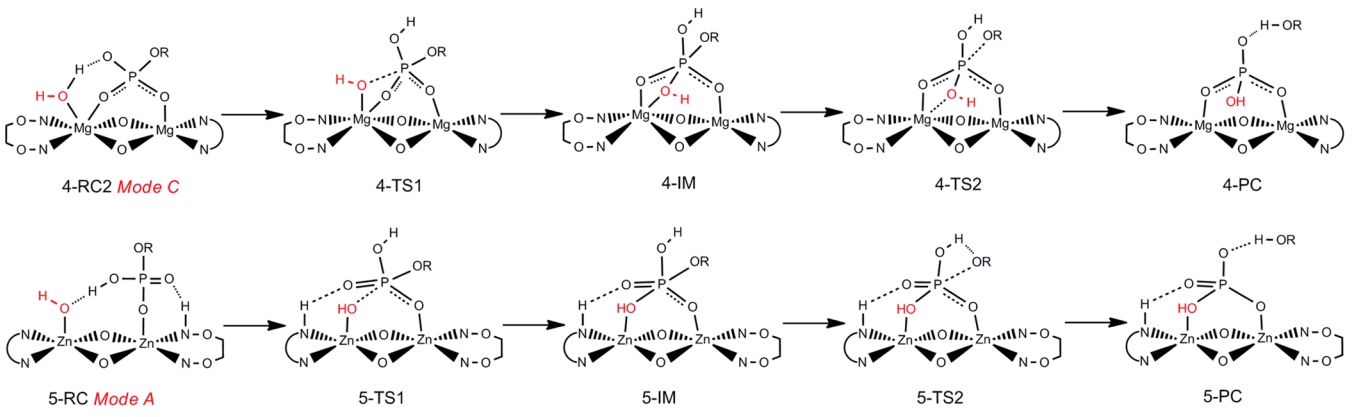

dx.doi.org/10.1021/ic402717x | Inorg. Chem. 2014, 53, 3354−3361

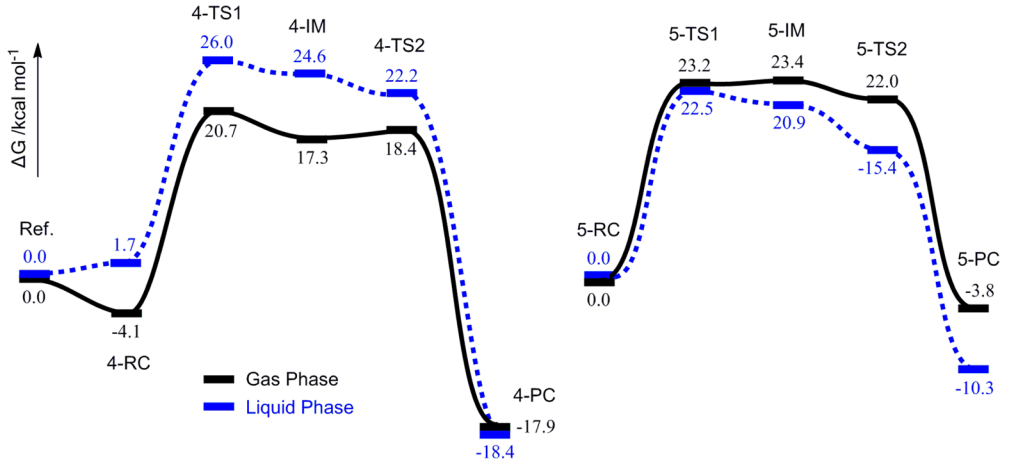

Figure 3. Relative free energy profiles of mechanisms 4 and 5. In mechanism 4, the relative free energies of the mode A based complex in both the gas phase and the liquid phase are set to zero and demonstrated as reference.

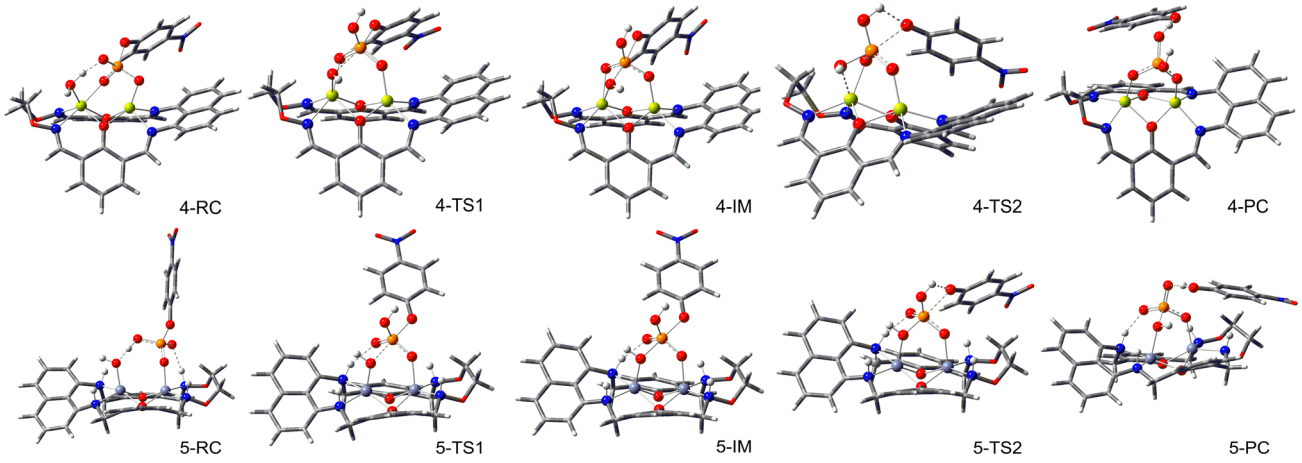

Figure 4. Optimized structures of the stationary reaction species in mechanisms 4 and 5.

Scheme 5. Alteration of the Intrinsic Rigidity of the Ligand by Replacing the Imine Groups with Amines

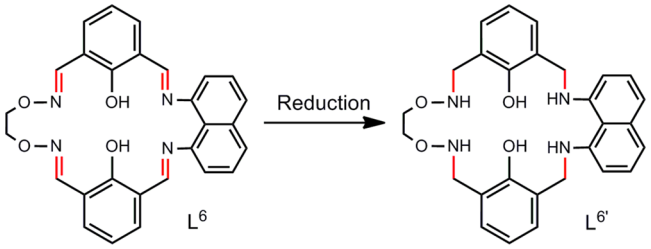

Mechanism 5 is also a stepwise S_N2-type addition–substitution pathway. The reactant **5-RC** is modeled based on mode A, and there is also a hydrogen bond formed between a phosphoryl oxygen atom and an amine-bound proton. This extra hydrogen bond helps the catalyst to better recognize and bind with the substrate. Similar to mechanism 4, **5-TS1** is featured by the nucleophilic attack, and a P–O bond to the leaving group is mainly cleaved in **5-TS2**. A slightly distorted trigonal bipyramidal phosphorane intermediate, **5-IM**, is also obtained along the reaction pathway.

Mechanism 4 is stepwise because there are more available coordination sites on the magnesium centers. What's the mechanistic benefit of mechanism 5 being stepwise? The answer can also be ascribed to more available coordination sites but on the second coordination sphere. Compared with the former ligand L6, each nitrogen atom in the less rigid ligand L6′ possesses a proton. A significant hydrogen bond between a phosphoryl oxygen and an amine-bound proton is maintained during the catalytic process, which helps to better stabilize the reaction complexes, and reasonably, a stepwise pathway is proposed in mechanism 5. Hence, noncovalent interactions between catalyst and substrate also help to stabilize the reaction intermediates.

It can be seen from Figure 3 that the reaction barrier of mechanism 5 is 22.5 kcal, and this is the lowest one among the five proposed mechanisms. What is the catalytic power of mechanism 5? Besides the function of the second coordination sphere, the intermetallic distances are also important (Table 2). As listed in Table 2, the O(Nu)---OPNP distances in transition

Table 2. Selected Structural Data from the Optimized Structures and Their Corresponding Relative Free Energies for the Dizinc Complex Catalyzed Hydrolysis of NPP^-

term	1-RC	1-TS	2-RC	2-TS	5-RC	5-TS
$Zn^{(II)}$---$Zn^{(II)}$ (Å)	3.13	3.02	3.13	3.03	2.98	2.84
O(Nu)---OPNP (Å)	3.68	2.60	3.31	2.64	3.17	2.58
ΔG (kcal/mol)	6.0	28.0	0.0	31.5	0.0	22.5

dx.doi.org/10.1021/ic402717x | Inorg. Chem. 2014, 53, 3354–3361

states **1-TS**, **2-TS**, and **5-TS** are very close (around 2.60 Å). The Zn---Zn distances in **1-TS** and **2-TS** are almost equal, while that in **5-TS** decreases sharply to 2.84 Å. The difference in the values between the Zn---Zn distance and O(Nu)---OPNP distance is the smallest among the three zinc-containing mechanisms, which means that the intermetallic distances of the dinuclear catalysts in mechanism 5 are beneficial to the binding with the substrate and the subsequent nucleophilic attack. Therefore, the decrease in the intrinsic rigidity of the ligand will lead to more flexibility in the coordination configurations of the metal centers, and the intermetallic distance will dynamically change to better bind with and catalyze the phosphate transfer reaction.

CONCLUSIONS

The hydrolysis mechanisms of phosphate monoester NPP^- promoted by unsymmetrical bivalent dinuclear complexes have been explored in this paper using DFT calculations. The form of the active catalyst has been verified, and the metal-bound hydroxyl ion acts as the nucleophilic reagent. The binding modes of the catalyst−substrate complexes were also explored, and four basic binding modes are proposed that considered one-point or two-point binding mechanisms, hydrogen bond networks, and whether the nucleophile is bridged or not. Two optional compartments for the location of the nucleophile-coordinated metal center are also investigated in order to explore the mechanistic differences in the unsymmetrical dinuclear complex catalyzed reactions.

Five plausible mechanisms were proposed in this computational study. Mechanisms 1, 2, and 3 employ an unsymmetrical dizinc complex. All of them are concerted S_N2 addition−substitution reaction pathways, and mechanism 1 is more competitive than the other two mechanisms. In mechanism 1, the nucleophile-coordinated zinc center is located in a compartment with more electronegative oxygen atom attached to the imine nitrogen atoms, and this facilitates the nucleophilic attack; therefore a concerted mechanism is observed. The activation free energy of mechanism 1 is 18.5 kcal/mol, and this value is close to the experimental value (19.6 kcal/mol). Therefore, the calculated results are consistent with the experimental observations and, more importantly, illuminate the mechanistic differences in the hydrolysis reactions catalyzed by the unsymmetrical dinuclear metal complexes.

Mechanisms 4 and 5 are proposed based on the selection of the metal centers and the intrinsic flexibility of the ligand. Both mechanisms 4 and 5 are stepwise S_N2-type reactions. The results here show that magnesium(II) ions with hard base properties and more available coordination sites are good candidates as a substitute in M^{II} dinuclear phosphatases. Meanwhile, the reaction energy barriers for the more distorted complexes are lower than those of the less distorted complexes.

The mechanistic differences between the concerted and the stepwise reaction pathways were also examined in this paper. We concluded that a better nucleophile, a good leaving group, and, more importantly, the presence of more available coordination sites (either from metal centers or from the functional second coordination sphere) are factors favorable for concerted mechanisms.

ASSOCIATED CONTENT

Supporting Information

Cartesian coordinates of optimized structures and the values of imaginary frequencies of corresponding transition states. The PES profiles of mechanisms 1, 2, 3, and 4 optimized with the basis sets 6-31G(d,p) (SDD for Zn). The figures of total energy along the intrinsic rection coordinate in each proposed mechanism. This material is available free of charge via the Internet at http://pubs.acs.org.

AUTHOR INFORMATION

Corresponding Author

*E-mail: ceszhcy@mail.sysu.edu.cn Fax: (+86) 84110523.

Notes

The authors declare no competing financial interest.

ACKNOWLEDGMENTS

We gratefully acknowledge the National Natural Science Foundation of China (Grant Nos. 21173273, 21373277, and J1103305) and the Research Grants Council of Hong Kong (Grant: HKU 7048/11P) for financial support. The research is also partially supported by the high-performance grid computing platform of Sun Yat-Sen University, the Guangdong Province Key Laboratory of Computational Science, and the Guangdong Province Computational Science Innovative Research Team.

REFERENCES

(1) (a) Westheimer, F. H. *Science* **1987**, *235*, 1173−1178. (b) Kamerlin, S. C. L.; Sharma, P. K.; Prasad, R. B.; Warshel, A. *Q. Rev. Biophys.* **2013**, *46*, 1−132.

(2) (a) Lipscomb, W. N.; Sträter, N. *Chem. Rev.* **1996**, *96*, 2375−2434. (b) Wilcox, D. E. *Chem. Rev.* **1996**, *96*, 2435−2458. (c) Weston, J. *Chem. Rev.* **2005**, *105*, 2151−2174. (d) Cleland, W. W.; Hengge, A. C. *Chem. Rev.* **2006**, *106*, 3252−3278.

(3) (a) Sharma, S.; Rauk, A.; Juffer, A. H. *J. Am. Chem. Soc.* **2008**, *130*, 9708−9716. (b) De Vivo, M.; Dal Peraro, M.; Klein, M. L. *J. Am. Chem. Soc.* **2008**, *130*, 10955−10962. (c) Elsässer, B.; Valiev, M.; Weare, J. H. *J. Am. Chem. Soc.* **2009**, *131*, 3869−3871. (d) López-Canut, V.; Roca, M.; Bertrán, J.; Moliner, V.; Tuñón, I. *J. Am. Chem. Soc.* **2010**, *132*, 6955−6963.

(4) (a) Chin, J. *Acc. Chem. Res.* **1991**, *24*, 145−152. (b) Krämer, R. *Coord. Chem. Rev.* **1999**, *182*, 243−261. (c) Molenveld, P.; Engbersen, J. F. J.; Reinhoudt, D. N. *Chem. Soc. Rev.* **2000**, *29*, 75−86. (d) Niittymaki, T.; Lonnberg, H. *Org. Biomol. Chem.* **2006**, *4*, 15−25. (e) Mancin, F.; Tecilla, P. *New J. Chem.* **2007**, *31*, 800−817. (f) Lonnberg, H. *Org. Biomol. Chem.* **2011**, *9*, 1687−1703. (g) Zhao, M.; Wang, H.-B.; Ji, L.-N.; Mao, Z.-W. *Chem. Soc. Rev.* **2013**, *42*, 8360−8375. (h) Maxwell, C. I.; Mosey, N. J.; Stan Brown, R. *J. Am. Chem. Soc.* **2013**, *135*, 17209−17222. (i) Gavrilova, A. L.; Bosnich, B. *Chem. Rev.* **2004**, *104*, 349−384.

(5) Lad, C.; Williams, N. H.; Wolfenden, R. *Proc. Natl. Acad. Sci.* **2003**, *100*, 5607−5610.

(6) (a) Kirby, A. J.; Varvoglis, A. G. *J. Am. Chem. Soc.* **1967**, *89*, 415−423. (b) Hengge, A. C.; Edens, W. A.; Elsing, H. *J. Am. Chem. Soc.* **1994**, *116*, 5045−5049. (c) Gahan, L. R.; Smith, S. J.; Neves, A.; Schenk, G. *Eur. J. Inorg. Chem.* **2009**, *2009*, 2745−2758.

(7) (a) Sadler, N. P.; Chuang, C.-C.; Milburn, R. M. *Inorg. Chem.* **1995**, *34*, 402−404. (b) Rawji, G. H.; Yamada, M.; Sadler, N. P.; Milburn, R. M. *Inorg. Chim. Acta* **2000**, *303*, 168−174. (c) Tafesse, F.; Deppa, N. C. *Ecotoxicol. Environ. Saf.* **2004**, *58*, 260−266. (d) Akl, J.; Ghaddar, T.; Ghanem, A.; El-Rassy, H. *J. Mol. Catal. A: Chem.* **2009**, *312*, 18−22. (e) Zulkefeli, M.; Suzuki, A.; Shiro, M.; Hisamatsu, Y.; Kimura, E.; Aoki, S. *Inorg. Chem.* **2011**, *50*, 10113−10123. (f) Coleman, F.; Erxleben, A. *Polyhedron* **2012**, *48*, 104−109. (g) Wang, Y.; Xiao, W.; Mao, J. W.; Zhou, H.; Pan, Z. Q. *J. Mol. Struct.* **2013**, *1036*, 361−371.

(8) (a) Retegan, M.; Milet, A.; Jamet, H. *J. Phys. Chem. A* **2010**, *114*, 7110−7116. (b) Kamerlin, S. C. L. *J. Org. Chem.* **2011**, *76*, 9228−9238. (c) Admiraal, S. J.; Herschlag, D. *J. Am. Chem. Soc.* **2000**, *122*,

2145−2148. (d) Rudbeck, M. E.; Blomberg, M. R. A.; Barth, A. *J. Phys. Chem. B* **2013**, *117*, 9224−9232. (e) Plotnikov, N. V.; Prasad, B. R.; Chakrabarty, S.; Chu, Z. T.; Warshel, A. *J. Phys. Chem. B* **2013**, *117*, 12807−12819. (f) Hou, G.; Cui, Q. *J. Am. Chem. Soc.* **2013**, *135*, 10457−10469.

(9) (a) Parimala, S.; Kandaswamy, M. *Transition Met. Chem.* **2004**, *29*, 35−41. (b) Thirumavalavan, M.; Akilan, P.; Kandaswamy, M. *Inorg. Chim. Acta* **2006**, *359*, 3831−3840. (c) Anbu, S.; Kamalraj, S.; Varghese, B.; Muthumary, J.; Kandaswamy, M. *Inorg. Chem.* **2012**, *51*, 5580−5592. (d) Anbu, S.; Kandaswamy, M. *Inorg. Chim. Acta* **2012**, *385*, 45−52. (e) Parimala, S.; Kandaswamy, M. *Inorg. Chem. Commun.* **2003**, *6*, 1252−1254.

(10) (a) Kamerlin, S. C. L.; Wilkie, J. *Org. Biomol. Chem.* **2007**, *5*, 2098−2108. (b) Klähn, M.; Rosta, E.; Warshel, A. *J. Am. Chem. Soc.* **2006**, *128*, 15310−15323.

(11) (a) Yun, J. W.; Tanase, T.; Lippard, S. J. *Inorg. Chem.* **1996**, *35*, 7590−7600. (b) Iranzo, O.; Richard, J. P.; Morrow, J. R. *Inorg. Chem.* **2004**, *43*, 1743−1750. (c) Feng, G.; Natale, D.; Prabaharan, R.; Mareque-Rivas, J. C.; Williams, N. H. *Angew. Chem.* **2006**, *118*, 7214−7217. (d) Linjalahti, H.; Feng, G.; Mareque-Rivas, J. C.; Mikkola, S.; Williams, N. H. *J. Am. Chem. Soc.* **2008**, *130*, 4232−4233. (e) Enthaler, S. *ACS Catal.* **2013**, *3*, 150−158.

(12) (a) Torres, R. A.; Himo, F.; Bruice, T. C.; Noodleman, L.; Lovell, T. *J. Am. Chem. Soc.* **2003**, *125*, 9861−9867. (b) Stec, B.; Holtz, K. M.; Kantrowitz, E. R. *J. Mol. Biol.* **2000**, *299*, 1303−1311. (c) Holtz, K. M.; Kantrowitz, E. R. *FEBS Lett.* **1999**, *462*, 7−11. (d) Yang, P.; Ren, R.; Guo, M.; Song, A.; Meng, X.; Yuan, C.; Zhou, Q.; Chen, H.; Xiong, Z.; Gao, X. *J. Biol. Inorg. Chem.* **2004**, *9*, 495−506.

(13) (a) He, C.; Lippard, S. J. *J. Am. Chem. Soc.* **1999**, *122*, 184−185. (b) Iranzo, O.; Kovalevsky, A. Y.; Morrow, J. R.; Richard, J. P. *J. Am. Chem. Soc.* **2003**, *125*, 1988−1993. (c) Bazzicalupi, C.; Bencini, A.; Bonaccini, C.; Giorgi, C.; Gratteri, P.; Moro, S.; Palumbo, M.; Simionato, A.; Sgrignani, J.; Sissi, C.; Valtancoli, B. *Inorg. Chem.* **2008**, *47*, 5473−5484.

(14) (a) Batista, S. C.; Neves, A.; Bortoluzzi, A. J.; Vencato, I.; Peralta, R. A.; Szpoganicz, B.; Aires, V. V. E.; Terenzi, H.; Severino, P. C. *Inorg. Chem. Commun.* **2003**, *6*, 1161−1165. (b) Jarenmark, M.; Csapo, E.; Singh, J.; Wockel, S.; Farkas, E.; Meyer, F.; Haukka, M.; Nordlander, E. *Dalton Trans.* **2010**, *39*, 8183−8194. (c) van Veggel, F. C. J. M.; Verboom, W.; Reinhoudt, D. N. *Chem. Rev.* **1994**, *94*, 279−299. (d) Collin, J.-P.; Dietrich-Buchecker, C.; Gaviña, P.; Jimenez-Molero, M. C.; Sauvage, J.-P. *Acc. Chem. Res.* **2001**, *34*, 477−487. (e) Subramanian, S.; Barclay, T. M.; Coulter, K. R.; McAuley, A. *Coord. Chem. Rev.* **2003**, *245*, 65−71.

(15) (a) Bazzicalupi, C.; Bencini, A.; Bianchi, A.; Fusi, V.; Paoletti, P.; Piccardi, G.; Valtancoli, B. *Inorg. Chem.* **1995**, *34*, 5622−5631. (b) Bazzicalupi, C.; Bencini, A.; Bianchi, A.; Fusi, V.; Giorgi, C.; Paoletti, P.; Valtancoli, B.; Zanchi, D. *Inorg. Chem.* **1997**, *36*, 2784−2790. (c) Jurek, P. E.; Jurek, A. M.; Martell, A. E. *Inorg. Chem.* **2000**, *39*, 1016−1020. (d) Bauer-Siebenlist, B.; Meyer, F.; Farkas, E.; Vidovic, D.; Dechert, S. *Chem.−Eur. J* **2005**, *11*, 4349−4360. (e) Mohamed, M. F.; Neverov, A. A.; Brown, R. S. *Inorg. Chem.* **2009**, *48*, 11425−11433.

(16) Frisch, M. J.; et al. *Gaussian 09*, Revision A.01; Gaussian, Inc.; Wallingford, CT, 2009.

(17) Gao, H.; Ke, Z.; DeYonker, N. J.; Wang, J.; Xu, H.; Mao, Z.-W.; Phillips, D. L.; Zhao, C. *J. Am. Chem. Soc.* **2011**, *133*, 2904−2915.

(18) (a) Becke, A. D. *J. Chem. Phys.* **1993**, *98*, 5648−5652. (b) Lee, C.; Yang, W.; Parr, R. G. *Phys. Rev. B* **1998**, *37*, 785−789.

(19) Dolg, M.; Wedig, U.; Stoll, H.; Preuss, H. *J. Chem. Phys.* **1987**, *86*, 866−872.

(20) (a) Fukui, K. *Acc. Chem. Res.* **1981**, *14*, 363−68. (b) Gonzalez, C.; Schlegel, H. B. *J. Phys. Chem.* **1990**, *94*, 5523−5527. (c) Gonzalez, C.; Schlegel, H. B. *J. Chem. Phys.* **1989**, *90*, 2154−2161.

(21) (a) Hratchian, H. P.; Schlegel, H. B. *J. Chem. Phys.* **2004**, *120*, 9918−24. (b) Hratchian, H. P.; Schlegel, H. B. *J. Chem. Theory Comput.* **2005**, *1*, 61−69.

(22) Tomasi, J.; Mennucci, B.; Cammi, R. *Chem. Rev.* **2005**, *105*, 2999−3094.

(23) The shape of the cavity in Bondi adopts interlocking spheres around atomic groups, while that in UFF uses interlocking spheres around each atom. Each hydrogen atom in Bondi and UFF has individual spheres (explicit hydrogens).

(24) Marenich, A. V.; Cramer, C. J.; Truhlar, D. G. *J. Phys. Chem. B* **2009**, *113*, 6378−6396.

(25) Humphry, T.; Forconi, M.; Williams, N. H.; Hengge, A. C. *J. Am. Chem. Soc.* **2002**, *124*, 14860−14861.

(26) Mechanism 2 is a stepwise pathway when optimized with the polarized basis set 6-31G(d,p) (SDD for Zn). However, the second transition state is no longer found (we cannot locate it although substantial searches for it were carried out) when optimized with diffused basis set 6-31+G(d,p) (SDD for Zn).